

Precision Laser Spectroscopy of the Ground State Hyperfine Splitting of Hydrogenlike $^{209}\text{Bi}^{82+}$

I. Klaft,¹ S. Borneis,² T. Engel,³ B. Fricke,⁴ R. Grieser,¹ G. Huber,¹ T. Kühl,² D. Marx,² R. Neumann,² S. Schröder,² P. Seelig,² and L. Völker³

¹*Institut für Physik, Universität Mainz, D-55099 Mainz, Germany*

²*Gesellschaft für Schwerionenforschung GSI, D-64220 Darmstadt, Germany*

³*Institut für Angewandte Physik, TH Darmstadt, D-64289, Darmstadt, Germany*

⁴*Institut für Physik, Gesamthochschule Kassel, D-34132 Kassel, Germany*

(Received 27 December 1993)

The first direct observation of a hyperfine splitting in the optical regime is reported. The wavelength of the $M1$ transition between the $F = 4$ and $F = 5$ hyperfine levels of the ground state of hydrogenlike $^{209}\text{Bi}^{82+}$ was measured to be $\lambda_0 = 243.87(4)$ nm by detection of laser induced fluorescence at the heavy-ion storage ring ESR at GSI. In addition, the lifetime of the laser excited $F = 5$ sublevel was determined to be $\tau_0 = 0.351(16)$ ms. The method can be applied to a number of other nuclei and should allow a novel test of QED corrections in the previously unexplored combination of strong magnetic and electric fields in highly charged ions.

PACS numbers: 32.30.Jc, 12.20.Fv, 35.10.Fk

The ground state of hydrogen and its heavier isotopes exhibit hyperfine structure (hfs) splitting caused by magnetic interaction of the $1s$ electron and the nucleus. This energy difference has been an important experimental and theoretical test ground for an improved understanding of nuclear structure [1] and quantum-electrodynamic (QED) effects [2]. In particular, the 1.4 GHz splitting frequency in hydrogen, corresponding to a wavelength of 21 cm, has been the subject of precision microwave spectroscopy [3–5], eventually providing the hydrogen maser with a relative frequency accuracy of 7×10^{-13} [6]. The extensive work on hydrogen hfs strikingly illustrated the potential for extending ground state hfs investigations to hydrogenlike ions. Nevertheless, microwave measurement of the $1s$ splitting in $^3\text{He}^+$ [7] has not been followed by further steps to higher- Z ions. This stagnation can be explained by the difficulty of producing and maintaining an ensemble of highly charged hydrogenlike ions that are suitable for precision measurements. In addition, with the increase of the hfs splitting energies proportional to Z^3 , these transitions are no longer accessible to microwave spectroscopy. In some cases, ground state hfs was reported to be observed in x-ray spectra recorded after electron capture from the K shell [8]. However, this could not be used for precision studies. Exceptional examples are found in muonic atoms, where the ground state hyperfine splitting has been measured to a precision of a few percent in ^{209}Bi [9] and $^{203,205}\text{Tl}$ [10].

We report here on the measurement of the ground state hfs splitting of hydrogenlike $^{209}\text{Bi}^{82+}$, the heaviest stable nuclide existing in nature. For heavy hydrogenlike ions, the wavelength of transitions between the ground state hfs components is shifted into the optical region accessible to laser spectroscopy [11]. The measurement was performed at the ESR heavy ion cooler storage ring at GSI [12]. Highly charged ions were produced with an efficiency of

about 30% by in-flight stripping of lower-charged bismuth ions accelerated to 200 MeV/nucleon in the heavy-ion synchrotron SIS. Hydrogenlike ions were then selected from the resulting charge state distribution and injected into the ESR storage ring. The high initial velocity spread of the ions was significantly reduced by electron cooling [13]. Since the beam lifetime in the storage ring was longer than one hour, it was possible to increase the beam intensity in the storage ring by accumulation of a number of cycles of the SIS. Up to 1.8×10^8 ions of $^{209}\text{Bi}^{82+}$ were stored at a velocity of $\beta = v/c = 0.58666(11)$. This value was deduced from the acceleration voltage of the electron cooler, which is determined with an absolute accuracy of 60 V, including the effects of space charge potentials. A relative velocity spread of $\delta\beta/\beta = 7 \times 10^{-5}$, measured by Schottky analysis of the signal induced in capacitive probes, was reached at the given beam intensity.

The experimental arrangement is shown in Fig. 1. The ion beam was overlapped in a collinear, antiparallel ($\theta = 180^\circ$) geometry with 10 mJ laser pulses of 30 ns duration from a dye laser pumped by an excimer laser. The alignment an overlap of the ion beam (8 mm diam) and the laser beam (10 mm diam) in a field-free straight section of the storage ring was controlled to an accuracy of 0.33 mrad by pairs of mechanical scrapers separated by 6 m. In this geometry the Doppler effect, according to

$$\lambda = \lambda_0 \frac{1}{\gamma(1 + \beta \cos\theta)},$$

with $\gamma = (1 - \beta^2)^{-1/2}$, shifts the required laser wavelength from $\lambda_0 = 250$ nm in the rest frame of the ions to $\lambda = 489$ nm in the laboratory frame at the given β . The velocity distribution of the circulating ions leads to a Doppler width of

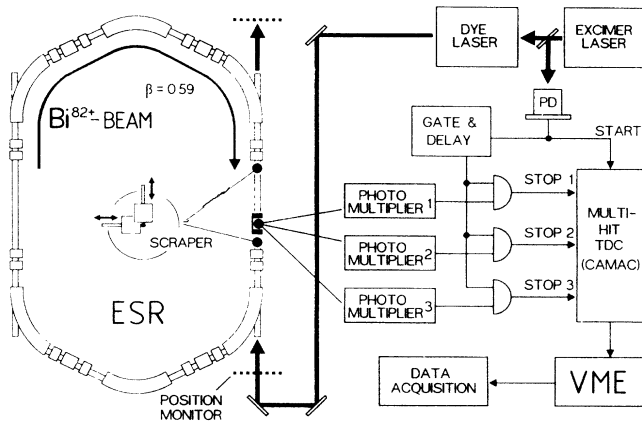


FIG. 1. Experimental arrangement: Hydrogenlike Bi^{82+} ions circulating in the ESR with an energy of 220 MeV/nucleon are excited by laser pulses from the $F = 4$ to the $F = 5$ hfs level in the ground state. Fluorescence is detected by three photomultipliers via an elliptical mirror.

$$\delta\nu = \nu\gamma^2\delta\beta,$$

which is 40 GHz in the laboratory frame of the conditions given above.

Because of the low transition probability, the $M1$ decay of the $F = 5$ sublevel takes place along the entire ESR orbit of 108.25 m. To collect fluorescence from a maximum solid angle, a 60 cm long cylindrical elliptical mirror system was installed in the ultrahigh vacuum beam tube of the storage ring. A fraction of 5×10^{-4} of the total emission in the ring is focused through sapphire windows on three photomultipliers outside of the vacuum. The Doppler effect causes a wide spectral distribution of the emitted light, ranging from 128 to 490 nm. Photons were accepted between the transmission cutoff of the sapphire windows at about 200 nm and the edge of a color-glass filter at 450 nm. This filter was necessary to suppress scattered laser light.

The detected fluorescence exhibits a time structure since only part of the ions in the ring can be excited by each laser pulse. This results in a modulation with the revolution frequency of the ions of 1.626 MHz corresponding to the revolution time of 615 ns. A time interval of 120 ns of signal is followed by about 495 ns, where ions not irradiated by the laser are passing the detector. This pattern is maintained throughout the decay time by virtue of the low velocity spread of the stored ions. In order to achieve an optimum suppression of stray light, the data taking electronics were triggered with a delay of $3 \mu\text{s}$ with respect to the laser pulse. The time information for every photon was recorded together with laser wavelength and intensity and the actual ion current in the ring. This allowed a software gating of the time intervals during which excited ions were passing the detector. In addition, it was possible to determine the lifetime of the excited hyperfine level with an efficient elimination of background.

A broad-band option for the dye laser was developed to enable a search over a wide wavelength region during the limited beam time available. The linewidth of the laser was increased to 120 GHz, compared with 4 GHz in the standard version, by replacing the grating with a prism as the tuning element [14]. After the line was first observed, the narrow-band option was reinstalled and used to produce the laser excitation spectrum shown in Fig. 2(a). The wavelength was calibrated by absorption spectroscopy in a ^{130}Te vapor cell [15].

The resonance was found at a laser wavelength of $\lambda = 477.794(4)$ nm. The quoted error is 10% of the Doppler width, which was 40 GHz as expected. The laboratory value λ corresponds to $\lambda_0 = 243.87(4)$ nm in the rest frame of the ions. The uncertainty in the rest frame value is indicated by the error bar in Fig. 2(a) and is dominated by the uncertainty in determination of the ion velocity in the ring $\frac{\Delta\beta}{\beta} = 1.9 \times 10^{-4}$, entering as

$$\Delta\lambda_0 = \lambda_0\beta\gamma^2\frac{\Delta\beta}{\beta}.$$

The effects of divergence and relative angle of the laser and ion beams are negligible compared to the velocity uncertainty.

The fluorescence decay curve acquired after the pulsed excitation is shown in Fig. 2(b). The extracted lifetime for an ion at rest, $\tau_0 = 0.351(16)$ ms, is about 15% shorter than given by [16]. It should be noted, however, that in addition to the quoted statistical error a reduction of the $F = 5$ lifetime by specific deexcitation processes in the storage ring cannot be completely excluded.

A complete theoretical evaluation of the hyperfine splitting is not presently available. Recent calculations [16,17] take into account the distributions of the extended nuclear charge and nuclear magnetization (Bohr-Weisskopf effect) but do not include contributions from QED. A transition wavelength between 242.3 and 244.8 nm is obtained, depending mostly on the particular treatment of

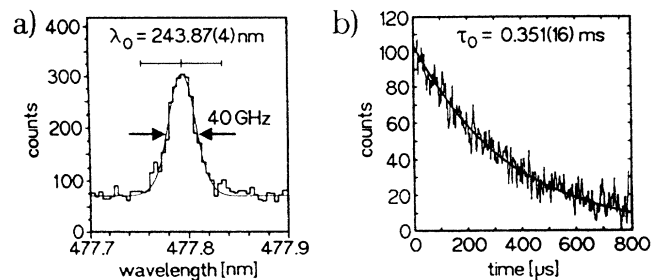


FIG. 2. (a) Resonance signal of the $M1$ transition in the ground state of $^{209}\text{Bi}^{82+}$. The Doppler width of the line is determined by the velocity spread of the stored ions. The error bar above the signal indicates the precision of the wavelength in the rest frame of the ions due to the uncertainty of the ion velocity. (b) Lifetime measurement of the $F = 5$ ground state hyperfine level of $^{209}\text{Bi}^{82+}$. The fluorescence is plotted as a function of the time decay with respect to the pulsed excitation.

the Bohr-Weisskopf shift, which has a total magnitude of about 6 nm.

Up to now, only the vacuum polarization (VP) term of the QED corrections has been calculated, resulting in a shift of -1.6 nm [17,18]. Calculations of the self-energy (SE) contributions in a combination of strong magnetic and electric fields are under way. Together with the above VP correction and the splitting energy calculated without QED, the experimental transition wavelength of 243.87(4) nm can be used to extract a range of values for the relative size of the SE and VP contributions. Ratios between $SE/VP = -0.4$ and -2 are obtained, differing substantially from $SE/VP \approx -4$ found in the computations of the Lamb shift in heavy hydrogenlike ions [19].

Presently, the experimental accuracy cannot be fully exploited due to uncertainty in the computation of the distribution of nuclear magnetism. Nuclei close to the double shell closure at ^{208}Pb , however, should exhibit a pronounced shell structure. In these favorable cases, semiempirical calculations reproduce the measured magnetic dipole moments with high precision [20]. Also, details of single-particle aspects of the nuclear charge distribution are well described by recent nuclear structure calculations in lead [21,22]. These successes support the assumption that calculation of the magnetic moment distributions should also reach a satisfying precision for these nuclei.

Since the new laser approach can be applied to a family of test cases, it will provide a sound experimental basis for the separation of nuclear and QED effects. The signal-to-noise ratio obtained for the resonance line clearly demonstrates the potential for extension to other, experimentally more demanding candidates. A straightforward application will be $^{207}\text{Pb}^{81+}$, where the main single-particle contribution is the unpaired neutron rather than the proton in $^{208}\text{Bi}^{82+}$. The different transition lifetimes of the upper hfs states of lead and bismuth will also address the problem of deexcitation in the ESR. Furthermore, measurements on lead can eliminate most of the uncertainty caused by the ion velocity. The Doppler-shifted laser wavelengths remain in accessible spectral regions for both parallel and antiparallel excitation. Thus, performing the experiment in both geometries simultaneously, the Doppler shift can be determined independently, allowing accuracy in the ppm region.

Suggestions of F. Bosch, H.-J. Kluge, and E.-W. Otten, and valuable discussions starting in the very early stage of the experiment are gratefully acknowledged.

We would like to thank M. Finkbeiner, M. Tomaselli, S. Schneider, and G. Soff for theoretical advice. The experimental success would have been impossible without the continuous cooperative effort of the members of the ESR group.

-
- [1] A. Bohr, Phys. Rev. **73**, 1109 (1948).
 - [2] S.J. Brodsky and G.W. Erickson, Phys. Rev. **148**, 26 (1966).
 - [3] J.E. Nafe and E.B. Nelson, Phys. Rev. **73**, 718 (1948).
 - [4] A.G. Prodell and P. Kusch, Phys. Rev. **88**, 184 (1952).
 - [5] P. Kusch, Phys. Rev. **100**, 1188 (1955).
 - [6] L. Essen, R.W. Donaldson, M.J. Bangham, and E.G. Hope, Nature (London) **229**, 110 (1971).
 - [7] H.A. Schuessler, E.N. Fortson, and H.G. Dehmelt, Phys. Rev. **187**, 5 (1969).
 - [8] G.L. Borchert, P.G. Hansen, B. Jonson, O.W. Schult, and P. Tidemand-Peterson, Phys. Lett. **63A**, 15 (1977).
 - [9] A. Rüetschi, L. Schellenberg, T.Q. Phan, G. Piller, L.A. Schaller, and H. Schneuwly, Nucl. Phys. **A422**, 461 (1984).
 - [10] H. Backe, R. Engfer, U. Jahnke, E. Kankeleit, R.M. Pears, C. Petitjean, L. Schellenberg, H. Schneuwly, W. U. Schroeder, H.K. Walter, and A. Zehnder, Nucl. Phys. **A189**, 472 (1972).
 - [11] T. Kühl, Phys. Scr. **T22**, 144 (1988).
 - [12] B. Franzke, Nucl. Instrum. Methods Phys. Res., Sect. B **24**, 18 (1987).
 - [13] B. Franke *et al.*, in *Proceedings of the 1993 Particle Acceleration Conference, Washington 1993*, (IEEE, Piscataway, 1993) p. 1645.
 - [14] T. Engel *et al.* (to be published).
 - [15] Jack Cariou and Paul Luc, *Atlas du spectre d'absorption de la molécule de tellure* (Laboratoire Aime Cotton CNRS II, Orsay, 1980).
 - [16] M. Finkbeiner, B. Fricke, and T. Kühl, Phys. Lett. **176A**, 113 (1993).
 - [17] S.M. Schneider, J. Schaffner, W. Greiner, and G. Soff, J. Phys. B **26**, L581 (1993).
 - [18] S.M. Schneider, W. Greiner, and G. Soff, Phys. Rev. A **50**, 118 (1994).
 - [19] W. Johnson and G. Soff, At. Data Nucl. Data Tables **42**, 189 (1985).
 - [20] K. Heyde, *The Nuclear Shell Model* (Springer-Verlag, Berlin, 1990).
 - [21] R.W. Hasse, B.L. Friman, and D. Berdichevsky, Phys. Lett. **181B**, 5 (1986).
 - [22] M.H. Sharma, G.A. Lalazissis, and P. Ring, Phys. Lett. **317B**, 9 (1993).